VIROLOGY 216, 174–183 (1996)
ARTICLE NO. 0044

Replication of Synthetic Defective Interfering RNAs Derived from Coronavirus Mouse Hepatitis Virus-A59

WILLEM LUYTJES,[1] HELEEN GERRITSMA, and WILLY J. M. SPAAN

Department of Virology, Institute of Medical Microbiology, Leiden University, 2300 AH Leiden, The Netherlands

Received September 27, 1995; accepted November 17, 1995

We have analyzed the replication of deletion mutants of defective interfering (DI) RNAs derived from the coronavirus mouse hepatitis virus (MHV)-A59 in the presence of MHV-A59. Using two parental DI RNAs, MIDI and MIDIΔH, a twin set of deletion mutants was generated with progressively shorter stretches of 5′ sequence colinear with the genomic RNA. All deletion mutants contained in-frame ORFs. We show that in transfected cells and after one passage the DI RNAs were detectable and that their accumulation was positively correlated with the length of 5′ sequence they contained. However, accumulation of two twin mutants, Δ2, in which sequences from nucleotide position 467 were fused to those from position 801, was undetectable. In passage 4 cells, but not in transfected or in passage 1 cells, recombination with genomic RNA led to the appearance of the parental DI RNAs. The accumulation of these parental RNAs was inversely correlated with the length of 5′ sequence on the deletion mutants and was highest in the Δ2 samples. In sharp contrast to the data reported for MHV-JHM-derived DI RNAs, we show that MHV-A59-derived mutant RNAs do not require an internal sequence domain for replication. The data suggest that coronavirus replication involves an RNA superstructure at the 5′ end of the genome or one comprising both ends of the genomic RNA. We also conclude from the recombination data that in-frame mutants with impaired replication signals are more fit than out-frame mutants with intact replication signals.

INTRODUCTION

Coronaviruses are enveloped animal viruses that cause diseases in livestock and pets and are among the agents of human common cold. They possess a positive-stranded RNA genome of 27–32 kb in a helical nucleocapsid form. The viral genes are expressed from a set of subgenomic (sg) mRNAs. Viral proteins are translated by a variety of strategies, including internal ribosomal entry, ribosomal frame shifting, and leaky scanning (Luytjes, 1995).

Replication and transcription of coronavirus RNA is a complex process that is not fully understood. After infection, a set of mRNAs of different lengths is synthesized. These RNAs consist of a "body" sequence, coterminal with the 3′ end of the genomic RNA, discontinuously fused to a leader sequence that is coterminal with the genomic 5′ leader (reviewed by Spaan *et al.,* 1988; Lai, 1990). Negative-stranded copies of the genome and the sg mRNAs are present in infected cells (Lai *et al.,* 1982; Baric *et al.,* 1983; Sethna *et al.,* 1989; Sawicki and Sawicki, 1990). The genomic minus strand is the template for amplification of the genome, but whether the sg minus strands play a role in the production of sg RNAs is currently under debate (for a recent review, see Van der Most and Spaan, 1995).

All viral RNAs produced in infected cells contain the same 5′ leader and the same 3′ end defined by the body sequence of the smallest mRNA. Progeny virions generally contain genomic RNA only, but some coronaviruses apparently can also package sg RNAs (Hofman *et al.,* 1990; Zhao *et al.,* 1993).

Study of coronavirus replication is impeded by the large size of the genomic RNA. No full-length cDNA clones are available of any coronavirus genome; thus reverse genetics on infectious clones is not possible. Therefore, several laboratories have focused on the analysis of defective interfering (DI) RNAs (Makino *et al.,* 1988; Van der Most *et al.,* 1991; Chang *et al.,* 1994). During coronavirus infection, DI genomes, deletion mutants of the genomic RNA, arise which are fully replication-competent and can be packaged into virions (Makino *et al.,* 1985; Van der Most *et al.,* 1991). These RNA molecules contain the essential signals for replication and packaging as does the genomic RNA but have the advantage of being of limited size. In the past years we and others have cloned naturally occurring DI RNAs of two strains of mouse hepatitis virus (MHV) to use in replication, transcription, and recombination studies (Van der Most *et al.,* 1991; Makino *et al.,* 1985). RNA transcripts of DI cDNA clones, after transfection into infected cells, are recognized by helper virus and replicated. Using synthetic DI RNAs, a specific signal necessary for packaging

[1] To whom correspondence and reprint requests should be addressed. Fax: (31)-71-5263645; E-mail: wluytjes@rullf2.LeidenUniv.nl; E-mail lab: azruviro@rulcri.LeidenUniv.nl.

0042-6822/96 $12.00

of DI RNA of MHV was mapped that is located approx 1.5 kb upstream of the POL ORF 1b termination codon (Fosmire *et al.,* 1992; Van der Most *et al.,* 1992).

The laboratories of both Lai and Makino delineated sequences necessary for replication of synthetic DI genomes derived from MHV-JHM by MHV-A59 helper virus (Kim *et al.,* 1993; Lin and Lai, 1993). A distinct feature of these replication signals was the requirement of an internal discontinuous sequence in addition to sequences at the termini of the DI genomes. In this paper we have analyzed in more detail the replication signals in a system using MHV-A59-derived DI RNAs and MHV-A59 as helper virus. We show that for replication in this homologous system the internal sequence element is obsolete and that a particular discontinuous fusion of sequences in the first 801 nucleotides from the 5′ end strongly inhibits its replication. The significance of these findings for the viral replication mechanism is discussed.

MATERIALS AND METHODS

Cells and viruses

Mouse L cells and 17Cl1 cells were grown in Dulbecco's modified Eagle's medium (DMEM) supplemented with 10% fetal calf serum (FCS). MHV-A59 was prepared on 17Cl1 cells in roller bottles in DMEM/3% FCS using a m.o.i. of 0.02. The virus was harvested 48 hr after infection and plaque titrated on L cells. Recombinant vaccinia virus vTF7.3 (Fuerst *et al.,* 1986) was grown on HeLa cells.

Recombinant DNA techniques

Standard recombinant DNA procedures were used (Sambrook *et al.,* 1989). Restriction enzymes, T4 DNA ligase, and T4 polynucleotide kinase were obtained from Gibco BRL. DNA sequence analysis was carried out using a sequencing kit (Pharmacia) and [α-^{33}P]dATP (NEN–Dupont). All enzyme incubations and biochemical reactions were performed according to the instructions of the manufacturers.

DNA transfection

A monolayer of L cells in a 35-mm dish was infected with vTF7.3 in DMEM/3% FCS using a m.o.i. of 10. After 1 hr of incubation at 37° and 5% CO_2 the cells were washed twice with PBS, lacking Mg and Ca. One microgram of unlinearized plasmid DNA was added to 100 μl DMEM and then mixed with 100 μl DMEM containing 10 μl lipofectin. The mixture was preincubated for 15 min at room temperature and the volume was adjusted to 1 ml with DMEM and added to cells. After 3 hr of incubation at 37° and 5% CO_2 the cells were washed once with PBS/DEAE and infected with MHV-A59 in PBS/DEAE/2% FCS using a m.o.i. of 10. After 1 hr of incubation at 37° and 5% CO_2 the inoculum was replaced by 600 μl of DMEM/10% FCS containing 10 μg actinomycin D (to inhibit vTF7.3 transcription). Seven hours after MHV infection viral RNA was isolated.

Isolation and analysis of viral RNA

Viral RNAs were isolated as described previously (Spaan *et al.,* 1981). RNAs were separated on 1% agarose gels containing 2.2 *M* formaldehyde and MOPS buffer [10 m*M* morpholinepropanesulfonic acid (sodium salt, pH 7), 5 m*M* sodium acetate, 1 m*M* EDTA]. Subsequently the gels were dried and hybridized to 100 ng of 5′-end labeled oligonucleotide (Van der Most *et al.,* 1991). Oligonucleotides were labeled using [γ-^{32}P]ATP (NEN–Dupont) and T4 polynucleotide kinase.

Construction of deletion mutants

Two series of deletion mutants were constructed, derived from pMIDI (Van der Most *et al.,* 1991) and pΔH-in (De Groot *et al.,* 1992). The latter is a deletion mutant of pMIDI (see Fig. 1).

Construction of pMIDI deletion mutants. To construct pMIDIΔPst the *Pst*I–*Pst*I fragment was removed from pMIDI which was religated in the presence of linker C112 (Table 1) to obtain an in-frame deletion mutant. Three polymerase chain reactions were carried out with pDISP (Van der Most *et al.,* 1995) as template: one using oligonucleotides C075 (covering the *Bam*HI site at nt 461, see Fig. 1) and C076 (linking nt 801 to a *Pst*I site), a second using oligonucleotides C077 (linking a *Bam*HI site to nt 801) and C078 (covering the *Pst*I site at nt 1140), and a third using oligonucleotides C075 and C091 (linking nt 983 to a *Pst*I site). The sequences of the oligonucleotides are represented in Table 1 and their positions are outlined in Fig. 1. The *Bam*HI–*Pst*I fragment in pMIDIΔPst was replaced by the respective PCR fragments digested with *Bam*HI and *Pst*I, yielding pMIDIΔ1, Δ2, and Δ3. The *Bam*HI–*Pst*I fragment was removed from pMIDI and replaced by linker C130 (Table 1) to obtain an in-frame pMIDIΔBam/Pst.

Construction of pMIDIΔH and deletion mutants. The *Bam*HI–*Pst*I fragment was removed from pΔH-in and replaced by the *Bam*HI–*Pst*I fragment from pMIDIΔ1, Δ2, and Δ3 yielding pMIDIΔHΔ1, Δ2, and Δ3, respectively.

Oligonucleotides

Oligonucleotides were synthesized on an Applied Biosystems 391 PCR MATE oligonucleotide synthesizer. A list of oligonucleotides used in this study is presented in Table 1.

RESULTS

The method of choice for studying replication signals of coronaviruses has been to make deletion mutants of

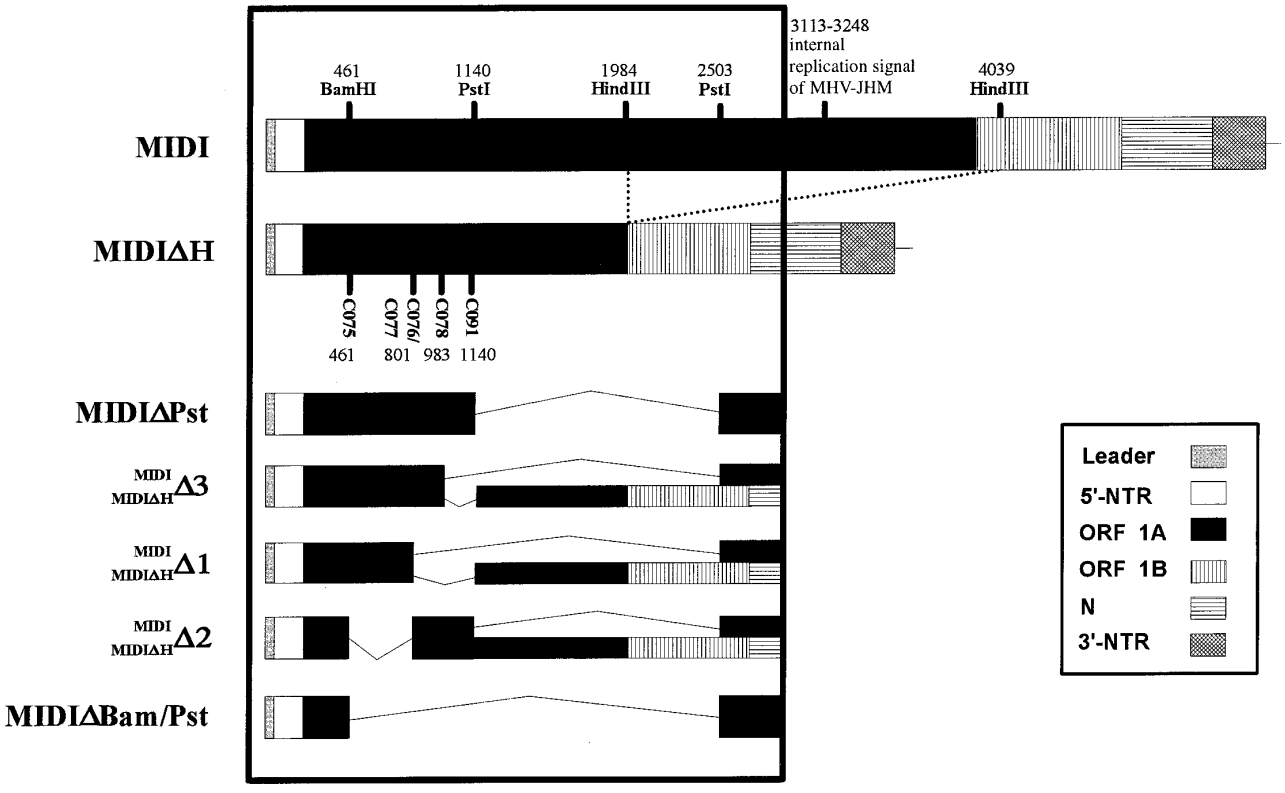

FIG. 1. Diagram of MHV-A59-derived DI RNAs and deletion mutants. Design of the DI RNAs is as indicated in the legend box. MIDIΔH is a deletion mutant of MIDI as outlined by the stippled lines. Above the diagram of the parental DI RNAs are indicated the relevant restriction sites and the position of the homologue of the internal replication signal of MHV-JHM. Below this diagram the PCR oligonucleotides (Table 1) used in the construction of the deletion mutants are indicated. The numbers represent the nt position from the 5′ end of MIDI RNA. For the deletion mutants only the relevant part is shown, outlined by the large box. The structure of the deletion mutants derived from the two different parental DI RNAs MIDI and MIDIΔH is represented by the thin boxes. Where the two groups are identical, thick boxes are used. Thin lines span the deleted regions.

cDNA clones of replicating DI RNAs (Makino *et al.,* 1988; Van der Most *et al.,* 1991). This approach was used by the laboratories of Lai and of Makino to study MHV-JHM DI replication by MHV-A59 (Kim *et al.,* 1993; Lin and Lai, 1993). The replication signals that emerged from their experiments were incompatible with the structure of one of the MHV-A59-derived MIDI subclones reported by us (Van der Most *et al.,* 1991; De Groot *et al.,* 1992). This suggests that a difference in replication signals between these closely related viruses may exist. To resolve this difference and to gain knowledge of MHV-A59 replication for our studies on recombination between MHV-A59 and synthetic RNAs, we set out to map 5′ replication signals on MIDI and derivatives.

TABLE 1

Oligonucleotides Used in This Study

Name	5′-sequence-3′	Purpose and location
C061	TCCGACGCGTAGAGCTTCATTACC	Hybridization to packaging signal in ORF 1b.
C075	TAGATGAGGATCCCCAGA	PCR (see Fig. 1).
C076	ACTCTGCAGCCCTTTGTTACCACCCT	PCR (see Fig. 1).
C077	CCGTGGATCCCAAAGGGTCTGTGACAT	PCR (see Fig. 1).
C078	TAGCAGTCTGCAGACGCA	PCR (see Fig. 1).
C091	TAGATACTGCAGACCATACTGGTCCACA	PCR (see Fig. 1).
C112	CCTC(T/A)GAGGTGCA	Linker.
C130	GATCCGGATGCTGCA	Linker.
C135	CGTCACTGGCAGAGAACG	Hybridization to 5′ NTR.
048	GTGATTCTTCCAATTGGCCATG	Hybridization to 3′ NTR.

Note. PCR, used for PCR cloning as described under Materials and Methods; linker, used for linker insertion as described under Materials and Methods.

We used two different parent DI RNAs for our deletion studies (see Fig. 1), MIDI (Van der Most *et al.,* 1991) and MIDIΔH (previously referred to as ΔH-in; De Groot *et al.,* 1992), which can be expressed from plasmids pMIDI and pMIDIΔH from an upstream T7 RNA polymerase promoter. These DI RNAs were selected because they are replicated efficiently by the viral polymerase. An identical series of deletions was introduced into the 5′-POL 1a part of both DIs. In this way a range of lengths of 5′ sequence colinear with the genome from 3889 (MIDI) through 1990 (MIDIΔH) to 466 nts (MIDIΔBam/Pst) was generated which could be analyzed in the background of differently sized DI genomes. For MIDI, in all cases but one (the Δ2 mutant), the 5′ sequences were fused to those starting at genomic nt position 2503. In the case of MIDIΔH all fusions except Δ2 were with sequences starting at position 1984. The structure of the DIs and of the deletions made are depicted in Fig. 1. Note that none of the MIDIΔH RNAs contain the internal sequence (nts 3113–3248 on the genomic RNA) reported to be required in *cis* for MHV-JHM DI replication by MHV-A59 (Kim *et al.,* 1993; Lin and Lai, 1993).

Since MHV-A59 DI RNAs, unlike most of those of MHV-JHM, need to contain long open reading frames to be detectable in cell lysates of transfected cells (De Groot *et al.,* 1992; Van der Most *et al.,* 1995), we generated the deletion mutants such that they contain a long ORF. The presence of the ORF was confirmed by *in vitro* translation of T7 RNA transcripts (data not shown). The replication of the deletion mutant RNAs was analyzed in transfected cells (P0) and after several passages (P1–4). P0 RNA was studied for two reasons. First, it could not be excluded that the deletions made would affect packaging or uncoating signals, in which case only the P0 data would directly reflect replication efficiency of the deletion mutants. Second, we have shown previously that DIs with reduced fitness will be out competed by recombinants with higher fitness upon passaging (De Groot *et al.,* 1992). Most deletion mutants we generated can revert to the parental DI RNA by recombination with genomic RNA. We expected that P0 DI RNA replication would probably be unaffected by competition with recombinant RNAs, but not DI RNA from further passages. We were interested in determining whether the mutant RNAs would have a reduced fitness because of the deletions, whether the recombinant parental DI RNAs would eventually prevail, and how the accumulation of the latter would relate to replication efficiencies of the deletion mutants.

L-cells were infected with vTF7.3 and MHV-A59 and subsequently transfected with equal amounts of unlinearized plasmid DNA as described under Materials and Methods. The vaccinia TF7.3 system produces high levels of RNA from transfected plasmids (Fuerst *et al.,* 1986). Seven hours after MHV-infection RNA was isolated and resolved on denaturing agarose gels. The gels were

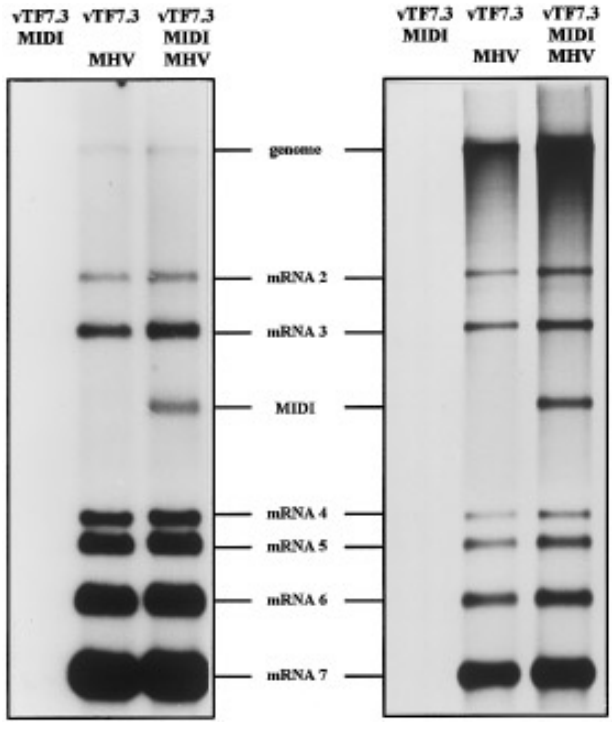

FIG. 2. Detection of MIDI RNA in L cells. (Left) Hybridization analysis of dried agarose gels containing RNA from lysates of L cells infected/transfected as indicated above the lanes. Oligo 048 (Table 1), which binds to the 3′ end of the genome, was used for hybridization. (Right) [^{3}H]Uridine labeling of RNA from L cells infected/transfected as indicated above the lanes.

dried and hybridized to oligonucleotide 048, which detects all viral RNAs, with c135, which binds to the 5′ NTR, or with c061, which binds to the packaging signal (Van der Most *et al.,* 1991; Fosmire *et al.,* 1992). The latter two oligonucleotides only detect DI and genomic RNA but give a background signal of ribosomal RNA (indicated by an asterisk in the figures). The T7-produced RNAs are not of one length as the transfected plasmids are not linearized and do not contain a T7 termination signal. However, the plasmids to include 20 nts of poly(A), which may cause the T7 polymerase to detach and could lead to the production of a population of RNAs of discrete length. To exclude that we would be detecting these RNAs in P0, instead of those produced by replication by the MHV polymerase, a control experiment was carried out first. Plasmid pMIDI was transfected into L-cells infected with vTF7.3 in the presence or absence of helper virus MHV-A59. Intracellular RNA was visualized using oligo 048. In Fig. 2 on the left it is shown that MIDI could not be detected in the absence of MHV-A59, thus its presence is the result of the addition of helper virus. Theoretically it could be possible that MHV-A59 merely provides factors that preserve the portion of T7-produced RNAs of DI length by protecting them from degradation. Metabolic labeling of RNA in the presence or absence of MHV-A59 and after shutdown of T7 transcription by

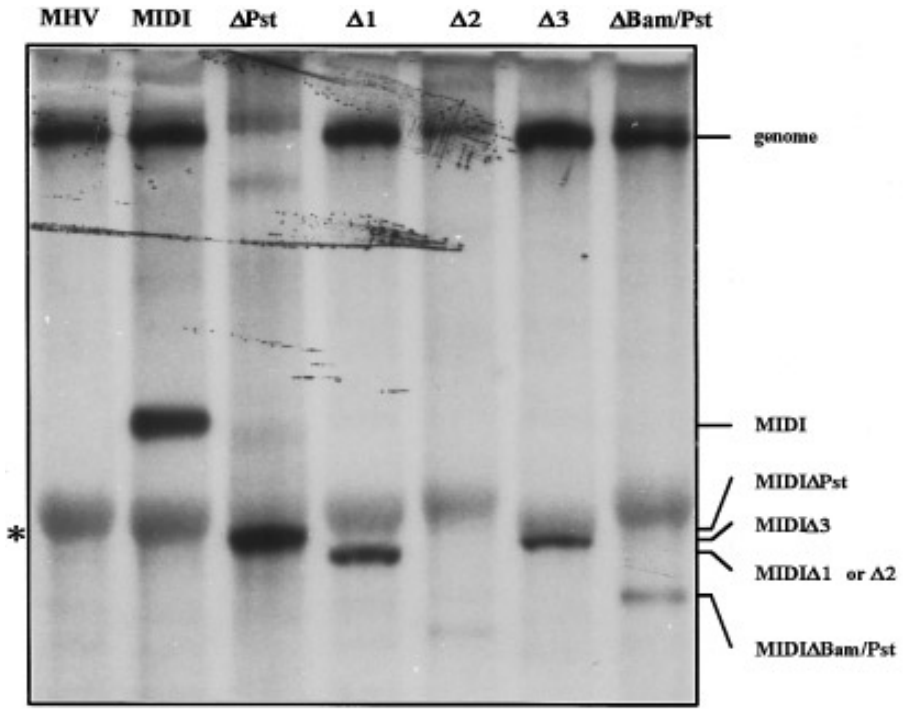

FIG. 3. Replication efficiency of MIDI and its deletion mutants in transfected L cells. Intracellular RNAs were harvested from L cells infected with vTF7.3 and MHV-A59 and transfected with plasmids encoding DI RNAs as indicated above the lanes. The RNA was separated on agarose gels, which were dried and hybridized to oligonucleotide C135, binding to the 5′ NTR. The positions of the deletion mutant RNA bands and of the MHV-A59 genomic RNA are shown at the right and the position of the 40S ribosomal RNA, nonspecifically binding to the oligonucleotide, is indicated by the asterisk at the left.

actinomycin D shows that this is not the case. The DI RNA MIDI was detected only when helper virus was present (Fig. 2, right).

We then went on to test each deletion mutant in L cells infected with vTF7.3 and MHV-A59 and transfected with the appropriate plasmids. The results, in transfected cells (P0), for each of the deletion mutant RNAs separated on agarose gels and hybridized to the 5′-NTR-specific oligonucleotide C135 (Table 1) are shown in Figs. 3 and 4.

Efficient replication was found for the two parental RNAs, although MIDIΔH, containing 1984 nts of genomic 5′ sequence, accumulated to lower levels than did MIDI. Figure 3 shows that MIDIΔPst (1145 nts) and mutants Δ3 (983 nts) and Δ1, lacking an additional 177 nts from the 5′ end, replicated efficiently, but to lower levels than the parental MIDI. The mutant MIDIΔBam/Pst, which has the shortest 5′ sequence (466 nts), clearly replicated poorly, but to detectable levels. From Fig. 4 it can be seen that the accumulation of the MIDIΔH derivatives was lower, but it showed the same pattern as did the MIDI derivatives. These mutants contain at most 1984 nts from the 5′ end of the genome. It thus follows that there is no need for the domain between genome nts 3113 and 3248, which is required for JHM DI replication (Kim *et al.,* 1993; Lin and Lai, 1993), to replicate MHV-A59-derived DI RNAs. Strikingly, the Δ2 mutants were

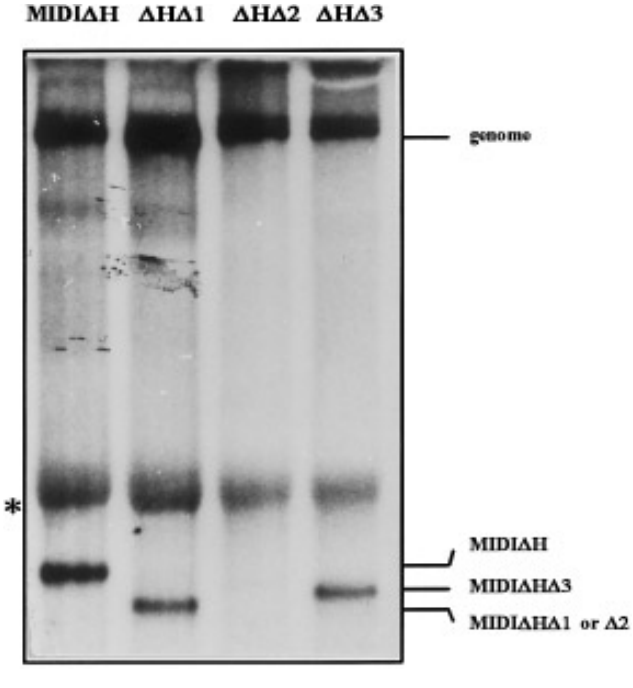

FIG. 4. Replication efficiency of MIDIΔH and its deletion mutants in transfected L cells. Agarose gels of intracellular RNA from L cells infected with vTF7.3 and MHV-A59 and transfected with plasmids encoding DI RNAs as indicated above the lanes were dried and hybridized to oligonucleotide C135. See also legend to Fig. 3.

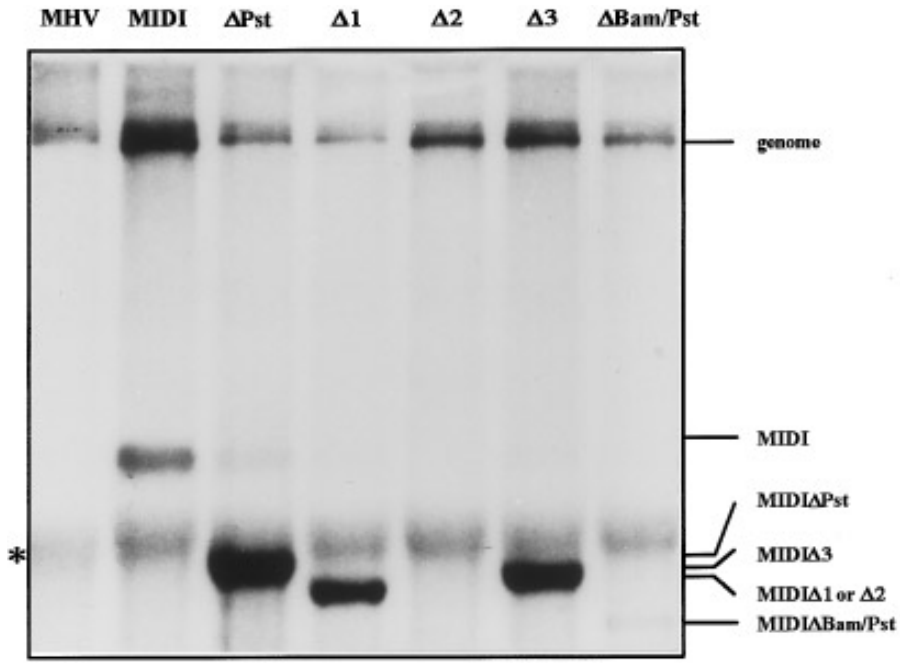

FIG. 5. Replication efficiency of MIDI and its deletion mutants in passage 1 L cells. Intracellular RNA, isolated 7 hr p.i. from L cells infected with DI viruses harvested from transfected cells (Fig. 3), as indicated above the lanes, was separated on agarose gels. These were dried and hybridized to oligonucleotide C135. See also legend to Fig. 3.

undetectable for both MIDI and MIDIΔH. These mutants have the same extent of 5′ sequence as does the ΔBam/Pst mutant. MIDIΔ2, instead of having its 5′ sequences fused to those from nt 2503 and on, as do all other MIDI deletion mutants, has additional sequences from nts 801 to 1144 discontinuously fused inbetween. It is thus a double deletion mutant. This is not the case with MIDIΔHΔ2, which is a single deletion mutant, with the deletion between nts 467 and 801. Densitometric scans of the autoradiograms showed that the replication efficiency of the deletion mutants in both series decreased with decreased length of 5′ sequences colinear with the genome (data not shown).

Next, virus, containing DI virus, was harvested from transfected and infected cells at 7 hr p.i. and used to infect fresh L cells. RNA was again harvested at 7 hr p.i. (P1 RNA) and separated on agarose gels. The results of hybridization of dried gels to 5′-NTR-specific oligonucleotide C135 are shown in Figs. 5 and 6.

The relative accumulation of P1 and P0 RNAs was essentially the same, showing that packaging and uncoating play no role in the replication of these RNAs. Again, the accumulation levels were lower when shorter stretches of 5′ sequence were present on the DIs. The deletion mutants of MIDI accumulated to somewhat higher levels than did MIDI. No clear recombination repair products were visible among the P1 RNAs, although a faint band of the approximate size of MIDI was visible in the MIDIΔPst lane.

To examine the fitness of the DIs further, we passaged the medium from the P1 cells three more times and analyzed the MIDI-derived RNAs of P2 and P4 (hybridized to oligo 048, which recognizes all viral RNAs) and the MIDIΔH RNAs of P4 (hybridized to oligo C061, which binds to the packaging signal) as described above (Figs. 7 and 8). Those DI RNAs seen to replicate in P0 and P1

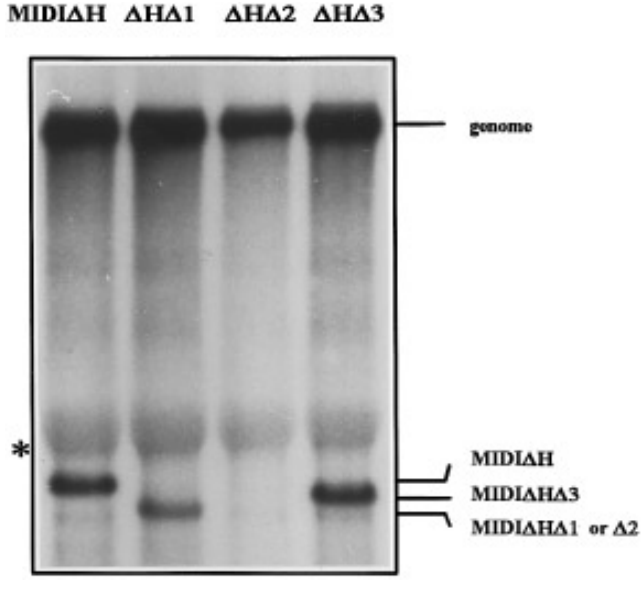

FIG. 6. Replication efficiency of MIDIΔH and its deletion mutants in passage 1 L cells. Agarose gels of intracellular RNA isolated 7 hr p.i. from L cells infected with DI viruses harvested from transfected L cells (Fig. 4) as indicated above the lanes. The gels were dried and hybridized to oligonucleotide C135. See also legend to Fig. 3.

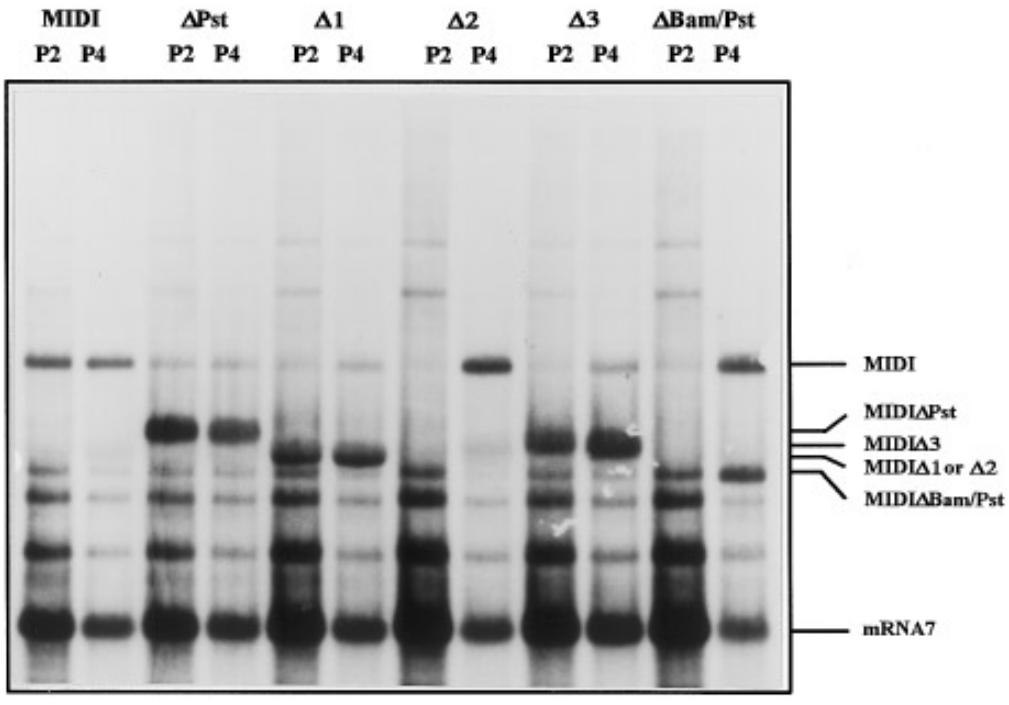

FIG. 7. Replication efficiency of MIDI and its deletion mutants in passage 2 and 4 L cells. DI viruses were passaged two (P2) to four (P4) times on L cells and intracellular RNA was analyzed on agarose gels. Dried gels containing RNA as indicated above the lanes were hybridized to oligonucleotide 048, which binds to the 3′ NTR.

continued to do so, but always the recombinant parental RNA emerged, although to very different levels. As for the MIDI derivatives (Fig. 7), the ΔBam/Pst and the Δ2 mutants clearly led to much higher levels of recombinant MIDI than did the other deletion mutants. Strikingly, it took four passages for the recombinant MIDI to emerge, particularly in the Δ2 samples. Densitometric scans were performed of the bands in P2 and P4 (data not shown). The intensity of the MIDI bands was unchanged in the ΔPst lanes and progressively increased from the Δ1 through the Δ3 mutants to the ΔBam/Pst and Δ2 deletion mutants, which showed an increase of four- to sixfold. Interestingly, this pattern is the reverse of that of the accumulation of the deletion mutants in the P0 and P1 passages.

The MIDIΔH mutants were only tested in a fourth passage, but behaved in a manner similar to that of the MIDI mutants. The parental RNA MIDIΔH was seen to appear in all three lanes of the deletion mutants (Fig. 8) but the levels in the Δ1 and Δ3 mutant lanes were much lower than that in the Δ2 lane. This is clearer from a lighter exposure in which the MIDIΔH and MIDIΔHΔ3 bands are better separated (data not shown).

DISCUSSION

Elucidation of the replication and transcription signals of coronaviruses is essential for a detailed understanding of the coronavirus life cycle. To date replication signals have only been studied for viruses of the MHV cluster of coronaviruses. In these viruses replicating DI RNAs naturally occur, which has opened the possibility of using recombinant DNA techniques on infectious cDNA clones to study the *cis*-acting sequences involved in virus replication and RNA transcription.

In this paper we describe the requirement of continuous stretches of 5′ sequence for replication by the MHV-A59 polymerase of MHV-A59-derived DIs. In contrast to the data reported by Kim *et al.* (1993) and Lin and Lai (1993) on replication signals of MHV-JHM DIs, an internal sequence domain (nts 3113–3248), which is present in MHV-A59 at the same position, is not necessary for replication of MHV-A59-derived DIs by MHV-A59 helper virus.

Replication efficiencies of the DI deletion mutants were reflected by the accumulation of the mutant DIs themselves in P0 and P1 intracellular RNA, but also by the accumulation of recombinant parental RNAs in the lysates of further passages. In fact, the length of 5′ sequences present on the deletion mutants was directly correlated with replication efficiency in P0 and P1 and, more interestingly, inversely correlated with the accumulation of parental recombinant RNA in P4. Thus, the replication efficiency of the deletion mutants was directly reflected in their fitness. We made sure at the outset of our experiments that the presence of an ORF would not be a factor in determining the fitness of the deletion mutants, by synthesizing all to contain a full-length ORF. Yet, the ORF would inevitably be of different length on the different deletion mutants. We have shown in earlier

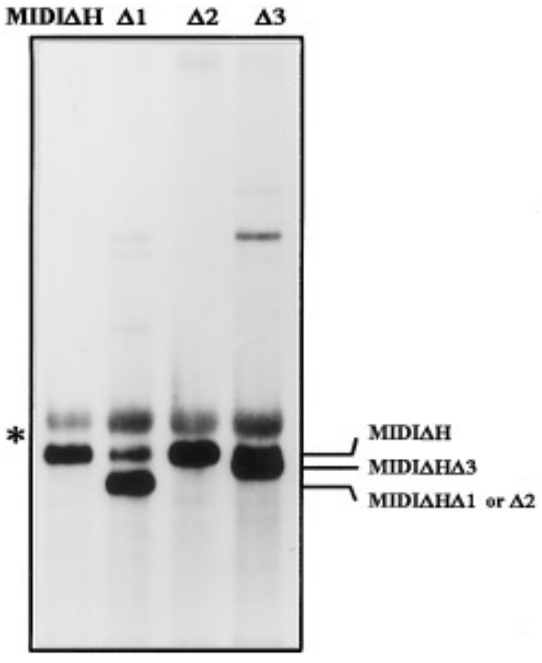

FIG. 8. Replication efficiency of MIDIΔH and its deletion mutants in passage 4 L cells. DI viruses were passaged four times on L cells and intracellular RNA was analyzed on agarose gels. Dried gels containing RNA as indicated above the lanes were hybridized to oligonucleotide C061, which binds to the packaging signal.

experiments that the length of the ORF may be a factor in determining the fitness of a DI RNA (Van der Most *et al.,* 1995). However, this is not the case in these deletion mutants: the MIDIΔBam/Pst mutant contains a longer ORF than MIDIΔH, yet replicates less efficiently. Also, the replication efficiency of the deletion mutants with the same 5′-end sequence but different length ORF is comparable.

We expected recombination and the generation of competing parental DI RNAs to become evident from passage 1 on, as we had seen in previous experiments. However, no parental DI RNA bands emerged in P1. The poorly replicating ΔBam/Pst mutant was not rapidly overgrown by the repaired and efficiently replicating recombinant MIDI RNA. More strikingly, the Δ2 mutants, which did not replicate to detectable levels at all, were not repaired by recombination to the parental DI RNAs in P1. This is remarkable since out-frame mutants are rapidly out competed by recombinant in-frame RNA: we have shown these to be already present in P0 and to prevail in P1 (Van der Most *et al.,* 1995). Recombinants did start to appear in P2 but only in the cases of the ΔBam/Pst and the Δ2 mutants did the recombinant parental DI clearly out compete the deletion mutants in P4. Apparently, the presence of an ORF on a DI RNA is a much stronger factor determining selection of recombination repair RNAs than is replication efficiency. In other words, a DI RNA containing a full-length ORF but with impaired replication signals is more fit than a DI RNA containing intact replication signals but with no full-length ORF. We are currently studying what underlying mechanism governs these different behaviors of DI RNAs.

The shortest length of 5′ sequences required for replication that could be mapped in our system was 466 nts. RNAs containing only these sequences at the 5′ end replicated poorly. This length is in the same range as that reported by Kim *et al.* (1993) for MHV-JHM and Chang *et al.* (1994) for BCV. Masters *et al.* (1994) showed that a synthetic RNA consisting of the mRNA7 sequence of MHV-A59 in which the leader was replaced by the 5′ 467 nts of the genomic RNA could be replicated. It was only detected after cocultivation of transfected and MHV-A59-infected L cells and 17Cl1 cells, thus not directly in P0 as in our system. The synthetic DI used by Masters *et al.* is modeled after a naturally occurring bovine coronavirus DI RNA, reported by Chang *et al.* (1994), which can be detected in transfected cells.

We have inserted the same range of deletions into the DISP RNA described earlier (Van der Most *et al.,* 1995). These deletion mutant RNAs replicate to much lower levels, but generally show the same pattern as the MIDI and MIDIΔH deletion mutants (data not shown). These DISP mutants contain 461 nts (poly(A) not included) from the 3′ end of the genomic RNA (Van der Most *et al.,* 1995), thus this constitutes the shortest length of 3′ sequence required for replication we have mapped on MHV-A59 DIs. The shortest 3′-replication signal on MHV-JHM RNA was mapped by Lin and Lai (1993) to be 436 nts.

Why is the replication efficiency of the deletion mutants correlated with the length of 5′ sequence it contains and why are the Δ2 mutants undetectable? The observations made with the latter provide an important clue about what factor may be involved. A fusion of the genomic nts 1–467 to 801 and further was not allowed in these mutants. The deleted sequence inbetween is by itself not required for replication, since it is also lacking in the ΔBam/Pst mutant, which replicates. All other deletion mutants contain fused sequences, yet none of these fusions were lethal. Thus, the lack of replication of the Δ2 deletion mutant RNAs seems to be the result of this particular joining of sequences. The key role is apparently played by the sequence domain between nts 468 and 800. It is not required for replication but is located in a region that is in some way involved in replication, since deletions in this region reduce replication efficiency. This interpretation leads us to speculate that coronavirus replication involves an RNA superstructure. If a secondary or tertiary structure of RNA plays some role in the replication cycle, reduction of the length of the sequences available for interaction would reduce the efficiency of replication to levels undetectable by our methods and ultimately would result in loss of replication. Conceivably, in the Δ2 mutants a joining of sequences is generated which disrupts the RNA superstructure such that replication is strongly impeded. We have analyzed

RNA folding in this region by computer and whether it is different for the different deletion mutants. A strong secondary structure is predicted, which comprises nts 110–470, both for positive- and negative-stranded RNA. This structure is different for the Δ2 mutants (not shown).

RNA structure at the 5′ end of genomic RNA being involved in replication or even constituting a replication signal is observed in an increasing number of plant and animal positive-strand RNA viruses. Among the more thoroughly studied of these are alphaviruses, containing a 5′ stem–loop structure involved in replication conserved in structure but not in sequence (reviewed by Strauss and Strauss, 1994); poliovirus, which requires a cloverleaf structure in the 5′-proximal 88 nts of genomic RNA for positive-strand RNA synthesis (Andino *et al.,* 1990); and the brome mosaic virus stem–loop structure with the same function (Pogue and Hall, 1992).

The minimal sequence length at the genomic 3′ end mapped to be required for MHV-A59 replication is 461 nts, which includes nucleocapsid protein coding sequences. As minus-strand synthesis alone appears dependent on the 55 terminal nts only (Lin *et al.,* 1994), the extended length of 3′ sequence required for replication may indicate that this part of the genomic RNA interacts with the 5′ structure to form a replication signal. This possibility is not without precedent: influenza viruses have terminal sequences that directly interact to form a panhandle structure, which plays a role in replication (Luo *et al.,* 1991; Fodor *et al.,* 1994). However, the putative interaction of coronavirus genomic termini would be completely different, since there are no sequence conservations or complementarities between the extreme ends of the genomic RNA. As yet, a role of RNA superstructures in coronavirus replication remains hypothetical. RNA secondary structure prediction programs are of limited reliability and prediction of RNA tertiary structure or long-range interactions are usually not supported. We are currently setting up experiments to analyze biochemically any involvement of RNA superstructures in coronavirus replication.

The features reported for the DI RNAs derived from MHV-A59 and MHV-JHM are remarkably different. A noted example is the observed difference in replication signals between MHV-A59 and -JHM DIs. In this paper and in previous reports we clearly show that for replication of MHV-A59-derived DI RNAs sequences beyond nt 1984 from the genomic 5′ end are obsolete. However, this observation remains in contrast to the data on MHV-JHM presented by other groups, where a domain between nts 3113 and 3248 is required for replication. More strikingly, Kim and Makino (1995) recently published an analysis of this 135-nt region that represents the *cis*-acting internal replication signal on JHM DI RNAs. They claim that it plays an essential role in plus-strand RNA synthesis, even for MHV-A59. These observations are in conflict with ours as reported here, but also with those reported by Masters *et al.* (1994), who have reported MHV-A59 DIs that also lack the *cis*-acting internal domain. It will be necessary to decide what is the basis of the difference in replication requirements between MHV-A59 and -JHM, for a better understanding of the replication of coronaviruses. Especially, it should be ruled out that obscuring factors such as host cells used for the experiments or individual differences in DI structure are at play. With respect to the first, the host cells used for the characterization of the deletion mutants of both viruses are different: the JHM-derived DIs were all tested in DBT cells, whereas we and Masters *et al.* (1994) performed the experiments in L cells or 17Cl1 cells.

When analyzing DI RNAs it should be kept in mind that the properties observed are not necessarily a true reflection of the properties and the replication characteristics of the genomic RNA. Whatever determines the differences between DIs, it remains possible that they are prone to display characteristics that have no relation to viral replication. Caution should thus be taken in extrapolating data generated with DI RNAs to the genomic RNA. A true study of the replication characteristics of the coronaviral genome will await an infectious clone and the use of reverse genetics.

ACKNOWLEDGMENTS

The authors thank Robbert van der Most, Guido van Marle, and Evelyne Bos for stimulating discussions. W.L. is supported by a grant from the Royal Dutch Academy of Sciences.

REFERENCES

Andino, R., Rieckhof, G. E., and Baltimore, D. (1990). A functional ribonucleoprotein complex forms around the 5′ end of poliovirus RNA. *Cell* 63, 369–380.

Baric, R. S., Stohlman, S. A., and Lai, M. M. C. (1983). Characterization of replicative intermediate RNA of mouse hepatitis virus: Presence of leader RNA sequences on nascent chains. *J. Virol.* 48, 633–640.

Chang, R. Y., Hofmann, M. A., Sethna, P. B., and Brian, D. A. (1994). A cis-acting function for the coronavirus leader in defective interfering RNA replication. *J. Virol.* 68, 8223–8231.

De Groot, R. J., Van der Most, R. G., and Spaan, W. J. (1992). The fitness of defective interfering murine coronavirus DI-a and its derivatives is decreased by nonsense and frameshift mutations. *J. Virol.* 66, 5898–5905.

Fodor, E., Pritlove, D. C., and Brownlee, G. G. (1994). The influenza virus panhandle is involved in the initiation of transcription. *J. Virol.* 68, 4092–4096.

Fosmire, J. A., Hwang, K., and Makino, S. (1992). Identification and characterization of a coronavirus packaging signal. *J. Virol.* 66, 3522–3530.

Fuerst, T. R., Niles, E. G., Studier, F. W., and Moss, B. (1986). Eukaryotic transient-expression system based on recombinant vaccinia virus that synthesizes bacteriophage T7 RNA polymerase. *Proc. Natl. Acad. Sci. USA* 83, 8122–8126.

Hofmann, M. A., Sethna, P. B., and Brian, D. A. (1990). Bovine coronavirus mRNA replication continues throughout persistent infection in cell culture. *J. Virol.* 64, 4108–4114.

Kim, Y. N., and Makino, S. (1995). Characterization of a murine coronavirus defective interfering RNA internal cis-acting replication signal. *J. Virol.* 69, 4963–4971.

Kim, Y. N., Jeong, Y. S., and Makino, S., (1993). Analysis of *cis*-acting sequences essential for coronavirus defective interfering RNA replication. *Virology* 197, 53–63.

Lai, M. M. (1990). Coronavirus: Organization, replication and expression of genome. *Annu. Rev. Microbiol.* 44, 303–333. [Review]

Lai, M. M. C., Patton, C. D., and Stohlman, S. A. (1982). Replication of mouse hepatitis virus: Negative-stranded RNA and replicative form RNA are of genome length. *J. Virol.* 44, 487–492.

Lin, Y. J., and Lai, M. M. (1993). Deletion mapping of a mouse hepatitis virus defective interfering RNA reveals the requirement of an internal and discontiguous sequence for replication. *J. Virol.* 67, 6110–6118.

Lin, Y. J., Liao, C. L., and Lai, M. M. (1994). Identification of the cis-acting signal for minus-strand RNA synthesis of a murine coronavirus: Implications for the role of minus-strand RNA in RNA replication and transcription. *J. Virol.* 68, 8131–8140.

Luo, G., Luytjes, W., Enami, M., and Palese, P. (1991). The polyadenylation signal of influenza virus RNA involves a stretch of uridines followed by the RNA duplex of the panhandle structure. *J. Virol.* 65, 2861–2867.

Luytjes, W. (1995). Coronavirus gene expression. *In* "The Coronaviridae" (S. G. Siddell, Ed.), pp. 33–54. Plenum, New York.

Makino, S., Fujioka, N., and Fujiwara, K. (1985). Structure of the intracellular defective viral RNAs of defective interfering particles of mouse hepatitis virus. *J. Virol.* 54, 329–336.

Makino, S., Shieh, C. K., Soe, L. H., Baker, S. C., and Lai, M. M. (1988). Primary structure and translation of a defective interfering RNA of murine coronavirus. *Virology* 166, 550–560.

Masters, P. S., Koetzner, C. A., Kerr, C. A., and Heo, Y. (1994). Optimization of targeted RNA recombination and mapping of a novel nucleocapsid gene mutation in the coronavirus mouse hepatitis virus. *J. Virol.* 68, 328–337.

Pogue, G. P., and Hall, T. C. (1992). The requirement for a 5′ stem–loop structure in brome mosaic virus replication supports a model for viral positive-strand RNA initiation. *J. Virol.* 66, 674–684.

Sambrook, J., Fritsch, E. F., and Maniatis, T. (1989). "Molecular Cloning: A Laboratory Manual," 2nd ed. Cold Spring Harbor Laboratory Press, Cold Spring Harbour, NY.

Sawicki, S. G., and Sawicki, D. L. (1990). Coronavirus transcription: Subgenomic mouse hepatitis virus replicative intermediates function in RNA synthesis. *J. Virol.* 64, 1050–1056.

Sethna, P. B., Hung, S. L., and Brian, D. A. (1989). Coronavirus subgenomic minus-strand RNAs and the potential for mRNA replicons. *Proc. Natl. Acad. Sci. USA* 86, 5626–5630.

Spaan, W. J. M., Cavanagh, D., and Horzinek, M. C. (1988). Coronaviruses: Structure and genome expression. *J. Gen. Virol.* 69, 2939–2952.

Spaan, W. J. M., Rottier, P. J. M., Horzinek, M. C., and Van der Zeijst, B. A. M. (1981). Isolation and identification of virus-specific mRNAs in cells infected with mouse hepatitis virus (MHV-A59). *Virology* 108, 424–434.

Strauss, H. S., and Strauss, E. G. (1994). The alphaviruses: Gene expression, replication, and evolution. *Microbiol. Rev.* 58, 491–562.

Van der Most, R. G., and Spaan, W. J. M. (1995). Coronavirus replication, transcription, and RNA recombination. *In* "The Coronaviridae" (S. G. Siddell, Ed.), pp. 11–32. Plenum, New York.

Van der Most, R. G., Bredenbeek, P. J., and Spaan, W. J. (1991). A domain at the 3′ end of the polymerase gene is essential for encapsidation of coronavirus defective interfering RNAs. *J. Virol.* 65, 3219–3226.

Van der Most, R. G., Heijnen, L., Spaan, W. J., and De Groot, R. J. (1992). Homologous RNA recombination allows efficient introduction of site-specific mutations into the genome of coronavirus MHV-A59 via synthetic co-replicating RNAs. *Nucleic Acids Res.* 20, 3375–3381.

Van der Most, R. G., Luytjes, W., Rutjes, S., and Spaan, W. J. (1995). Translation but not the encoded sequence is essential for the efficient propagation of the defective interfering RNAs of the coronavirus mouse hepatitis virus. *J. Virol.* 69, 3744–3751.

Zhao, X., Shaw, K., and Cavanagh, D. (1993). Presence of subgenomic mRNAs in virions of coronavirus IBV. *Virology* 196, 172–178.